

搅拌针偏心距对焊缝金属塑性流动行为的影响

毛育青^{1,2}, 柯黎明^{1,2}, 刘奋成¹, 刘 强²

(1. 南昌航空大学 轻合金加工科学与技术国防重点学科实验室,南昌 330063;

2. 西北工业大学 凝固技术国家重点实验室,西安 710072)

摘 要: 采用搅拌针偏心距分别为0.1 0.2 0.3 0.4 mm 搅拌头对叠层进行焊接试验,分析其对焊缝金属塑性流动行为影响。结果表明,焊缝由轴肩区、紊流区、焊核区及挤压区组成,其中紊流区为焊核区和轴肩区挤压金属形成的结果,前进侧挤压区金属变形尺寸明显大于返回侧。随偏心距增加,焊核区面积、宽度及挤压区标示材料向上迁移高度先增大后减小,前进侧标示材料向上迁移距离大于返回侧。由0.2 mm 偏心距搅拌头获得焊核区面积和标示材料向上迁移距离最大。但焊核区宽度最大焊缝由0.3 mm 偏心距搅拌头获得。根据焊缝金属塑性流动形态,提出搅拌针波动式挤压物理模型。

关键词: 搅拌摩擦焊; 偏心距; 塑性流动; 波动式挤压模型

中图分类号: TG 453.9 文献标识码: A 文章编号: 0253-360X(2017)02-0051-06

0 序 言

搅拌摩擦焊(friction stir welding, FSW)是一种新型的固态连接技术,其实质是通过高速旋转搅拌头与被焊工件搅拌、摩擦产热使金属达到塑性状态,发生充分流动而形成致密焊缝。焊接时母材金属不熔化,可避免传统熔焊过程中形成的焊接裂纹、气孔等缺陷,接头质量高,已被广泛应用于铝、镁及其合金等金属焊接^[1-3]。

研究表明,搅拌摩擦焊缝成形与金属塑性流动行为密切相关,直接影响接头性能。如何获得最佳的焊缝金属流动形态,提高接头质量是急需解决的关键问题。影响搅拌摩擦焊缝金属塑性流动的因素很多,其中搅拌头形状对金属流动起着最重要的作用^[4]。柯黎明等人^[5]研究发现,采用带反螺纹搅拌针焊接时有利于焊缝上部塑化金属向下迁移;王晓东等人^[6]认为,增加搅拌针螺纹数可增大塑性金属的向下迁移驱动力及迁移量。与无偏心距搅拌头相比,采用偏心式搅拌头可扩大搅拌头旋转占用空间体积与搅拌针本身空间体积的比值,使热塑性金属更易围绕搅拌针流动。Thomas等人^[7]首次证实采用偏心式搅拌头能促使更多不可压缩的塑化金属围绕搅拌针运动;Khodaverdizadeh等人^[8]发现偏心距越

大,搅拌针脉动搅拌作用越剧烈,反而使焊缝组织容易粗化,降低接头力学性能;Mao等人^[9]研究发现,随着搅拌针偏心距增大,接头强度呈先增大后减小趋势。但是关于搅拌针偏心距大小对焊缝金属塑性流动形态的具体影响还未见报道。

基于上述研究结果,采用镶嵌标示材料方法来观察焊后焊缝中标示材料的流动轨迹,分析搅拌针偏心距对金属流动影响。为加深对搅拌摩擦焊成形机理解及搅拌头的合理设计提供理论指导。

1 试验方法

采用偏心距(用 R 表示偏心距大小)分别为0.1 0.2 0.3 及0.4 mm的搅拌头进行焊接试验,其示意图如图1所示,搅拌头型号 N 分别为1 2 3 4。为保证加工精度,使用XK7132SD型精密数控铣床加工搅拌头,误差控制在允许范围内。搅拌头加工材料为GH4169高温合金,轴肩端面为内凹形,直径为28 mm;搅拌针形状为左螺纹圆锥形,根部直径为10 mm,端部直径为5 mm,长度为9.7 mm,搅拌针螺距为1.5 mm。

试验材料选用厚度为1和2 mm的LY12铝合金薄板作为基材,0.02 mm厚的铜箔片作为标示材料,交替叠放在基材之间。图2为标示材料镶嵌示意图。其中图2a为标示材料平行于焊缝表面镶嵌,最上表面和下表面为2 mm厚的LY12铝合金,中间交替叠放1 mm的LY12和0.02 mm的铜箔,形成铝

收稿日期: 2015-01-16

基金项目: 国家自然科学基金资助项目(51265043);江西省高等学校科技落地计划资助项目(KJLD13055, KJLD12074)

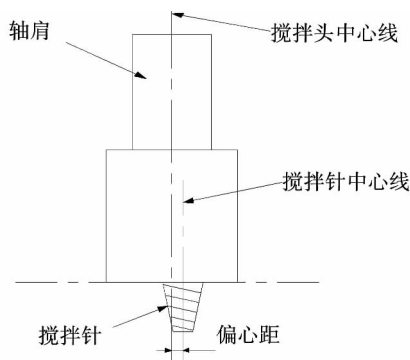


图1 带偏心距的搅拌针示意图

Fig. 1 Schematic of tool pin with an eccentricity

合金和铜箔相间的叠层结构,整个叠层厚度为 10.02 mm. 图 2b 为标示材料平行于焊接方向叠放,每块标示材料高度为 10 mm,整个叠层保持 0.02 mm 铜箔和 1 mm 的 LY12 交替叠放,叠层宽度约为 30.2 mm,叠层外侧用 LY12 铝合金固定夹紧.

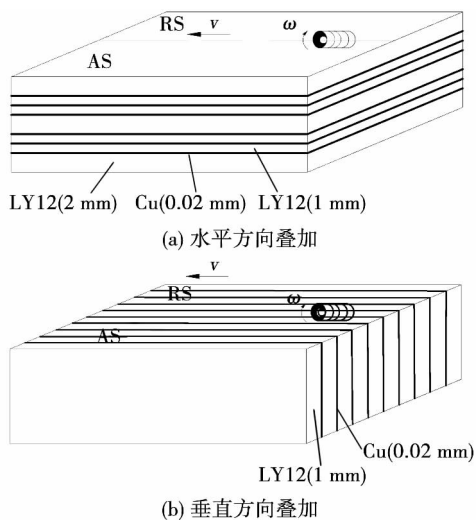


图2 标示材料叠放位置示意图

Fig. 2 Schematic of arranged position of insert tracer material

焊接设备为 X35K 型立式铣床改装的搅拌摩擦焊机. 焊接时搅拌头作顺时针旋转,工艺参数统一为搅拌头转速 750 r/min,焊接速度 60 mm/min,倾斜角 2° ,下压量为 0.5 mm. 焊后观察标示材料分布状态,分析焊缝塑性金属的流动行为.

2 结果与讨论

2.1 焊缝横截面形貌特征

图 3 为使用带 0.2 mm 偏心距搅拌头焊接时获得的焊缝横截面形貌. 图 3 中 AS(advancing side, 简

称 AS) 表示焊缝前进侧,RS(retreating side, 简称 RS) 表示焊缝返回侧,白色虚线表示焊缝中心线,黑色虚线表示焊缝各区域的轮廓线,最外围虚线圈住的范围表示焊缝变形区. 由图 3 可见,变形区呈上宽下窄形状,两侧标示材料发生明显向上弯曲变形. 焊缝中心处的标示材料被充分搅碎,呈弥散分布. 焊缝横截面被划分为 4 个特征区域,最表层类似于“漏斗”形区域为轴肩区,塑性材料呈扁平状分布. 轴肩区下方可见明显的弥散状标示材料,此区域为紊流区. 最下方的呈椭圆形分布的区域为焊核区,内部存在明显的“洋葱环”,被搅碎的标示材料沿洋葱环呈一定规律排列. 焊核区两侧为挤压区,但并不沿焊缝中心线对称,前进侧挤压区尺寸大于返回侧.

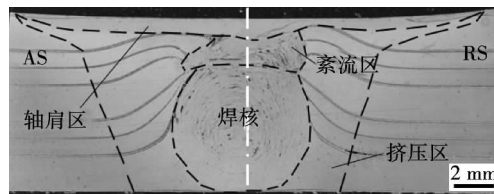


图3 焊缝横截面形貌

Fig. 3 Cross section of weld

分析认为,焊接时金属与高速旋转的轴肩端面直接接触,摩擦生热使温度迅速升高而立刻被塑化,受轴肩外围冷金属阻碍作用而无法向四周迁移. 此外轴肩端面为凹面形,在黏着力带动下塑化金属进入凹面内并向中心迁移,在轴肩内弧面的挤压力作用下沿搅拌针表面螺纹向下迁移. 随着距焊缝表面距离增加,轴肩作用效果逐渐减弱而导致轴肩区形成如图 3 中所示的漏斗状.

由“抽吸-挤压”理论可知^[10],焊缝上部塑化金属受搅拌针表面螺纹作用向下流动,并在搅拌针端部流出. 而受垫板刚性约束时转而向上迁移,并最终在轴肩顶锻力作用下而停止往上迁移. 与此同时,受搅拌针剪切挤压作用,其前方部分塑化金属随搅拌针旋转挤压而沿其两侧向其后方空腔迁移,并和往上迁移的塑化金属汇聚结合,形成中心靠近底板的球状区域. 随着搅拌头向前移动,此球状区域也随之前移,在搅拌头后方留下一个个球形叠加区,形成如图 3 所示的洋葱环状焊核区. 两侧挤压区变形金属水平轧制流线向上弯曲是由于受到来自焊核区挤压作用而向上迁移. 焊缝金属迁移至底部时受垫板刚性阻碍,转而对周边金属产生挤压作用,远离焊缝中心的母材金属温度较低,抗变形能力大,阻碍塑化金属继续迁移. 由于焊缝表面金属温度较高,

其变形抗力更低, 变形金属开始向抗力低的焊缝表面迁移. 当到达焊缝上部时, 受到轴肩顶锻作用而不再向上迁移, 前进侧和返回侧两侧迁移上来的金属最终在焊核区上方汇聚, 形成混合叠加的“紊流区”. 前进侧挤压区尺寸比返回侧大是由于焊接时两侧金属流动方向不同. 搅拌头前移时, 前进侧部分金属向其后方流动并对母材产生挤压, 返回侧部分金属顺着搅拌针旋转方向流到前进侧并挤压母材金属, 导致前进侧挤压区尺寸大于返回侧.

2.2 对塑性金属沿厚度方向上迁移的影响

图 4 为焊缝横截面宏观形貌, 其中 H_a 和 H_r 分别表示前进侧和返回侧标示材料向上迁移最大高度, W_{NZ} 表示焊核区最大宽度, A_{NZ} 表示焊核区面积.

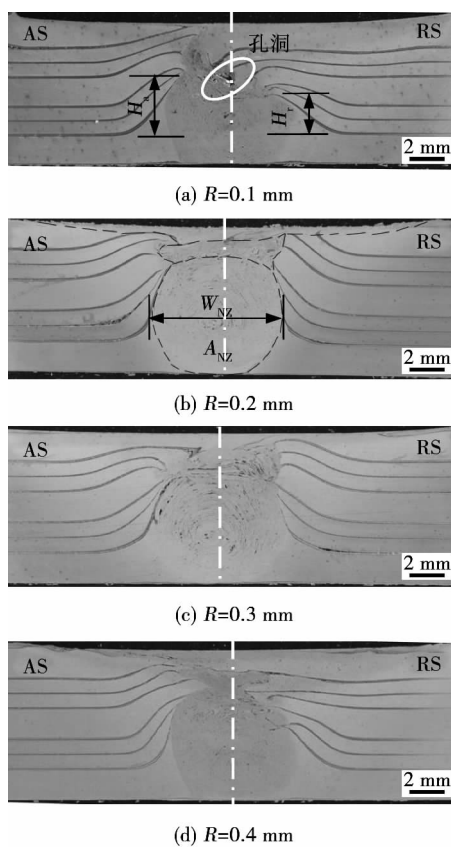


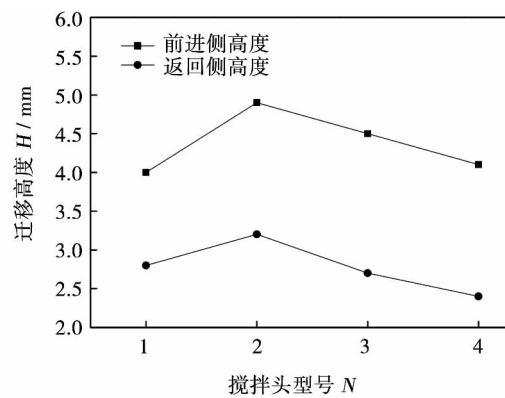
图 4 不同偏心距搅拌头下获得的焊缝横截面形貌(沿厚度方向)

Fig. 4 Cross sections of welds produced by tool pins with different eccentricities(along thickness direction)

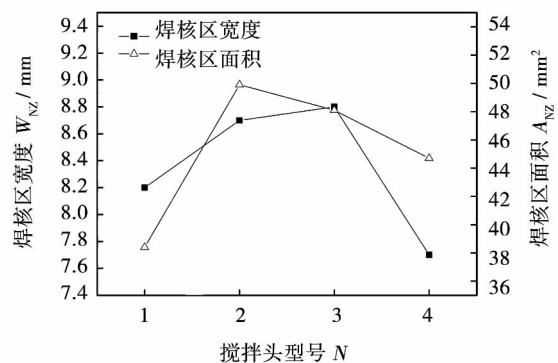
由图 4 可见, 各焊缝形貌及其尺寸相差较大, 在前进侧, 焊核区塑化金属挤压周边母材及标示材料从焊缝底部开始向上迁移, 距离焊缝表面越近, 流线弯曲程度越小. 向上弯曲的流线靠近轴肩区时, 受轴肩挤压作用转而向焊缝中心线延伸. 在返回侧, 标示材料弯曲情况与前进侧类似, 不同之处在于返

回侧靠近焊缝表面流线向紊流区延伸更多, 且返回侧标示材料向上迁移最大高度明显低于前进侧. 图 4a 中焊缝紊流区出现了明显的孔洞, 这是由于焊核区金属挤压周围金属向上迁移量不足造成的.

为进一步描述偏心距大小对焊缝金属流动行为的影响程度, 对标示材料迁移高度及焊核区尺寸进行精确测量. 图 5a 表示为标示材料向上迁移距离变化曲线, 图 5b 则表示为焊核区面积及最大宽度变化曲线. 由图 5a 可见, 各焊缝前进侧标示材料向上迁移高度均大于其返回侧的; 随偏心距增加, 标示材料向上迁移高度呈先增大后减小的趋势; 采用 2 号搅拌头焊接时标示材料向上迁移高度最大, 分别为 4.9 和 3.2 mm. 由图 5b 可见, 随偏心距增加, 焊核区面积和宽度也呈先增加后减小趋势; 采用 2 号搅拌头焊接时获得的焊缝焊核区面积最大, 约为 49.9 mm^2 ; 但是焊核区宽度最大的却是由 3 号搅拌头获得, 约为 8.8 mm.



(a) 两侧标示材料向上迁移高度



(b) 焊核区宽度和面积

图 5 搅拌针偏心距对焊缝各尺寸的影响

Fig. 5 Effect of pin eccentricities on different weld sizes

分析发现, 搅拌摩擦焊接过程中, 焊缝返回侧金属温度高于前进侧^[11], 变形抗力更低, 金属对焊核区塑化金属的横向阻力小于前进侧, 焊核区金属

在横向迁移量的增加导致变形金属向上迁移高度下降,最终导致返回侧金属最大迁移高度小于前进侧的。理论上,搅拌针偏心距越大,搅拌头旋转时占用空间体积越大,被搅碎的金属量越多,向下迁移金属量越多,焊核区面积和宽度越大,但实际情况并非如此。当偏心距较小时,搅拌针剪切金属量较少,没有更多的金属填充搅拌头后方的空腔,就会出现如图 4a 中的孔洞。随着偏心距增加至 0.2 mm 时,搅拌针的搅拌效果增强,更多的塑化金属填充搅拌头后方的空腔,且对周边的金属挤压效果更好,金属流动更充分,焊核区尺寸随之增大。而当偏心距增至 0.4 mm 时,搅拌针对焊缝金属的搅拌作用过于剧烈,单位时间内搅拌头与焊缝摩擦产热过大,使得焊缝上部金属温度过高,金属急剧软化,搅拌针带动塑化金属向下迁移量降低。而底部金属温度较低,使得搅拌针端部周围金属无法挤压周边金属,而更容易沿着搅拌针表面向上流动。同时焊缝上部金属温度较高,搅拌针与周围金属易由粘着摩擦转为滑动摩擦^[9],金属粘度较低,搅拌针挤压塑化金属向其后方空腔中迁移的金属量减少,与焊缝下部汇聚的塑化金属总量降低,导致底部焊核区面积和宽度减小。

2.3 对塑性金属在水平方向上迁移的影响

图 6 为标示材料平行焊接方向叠加时获得的焊缝横截面形貌。图 6c 中 F_1 、 F_3 表示焊核区金属对周边变形金属的挤压力, F_2 、 F_4 表示周边冷金属对焊核区塑化金属的反作用力。由图 6 可见,被充分塑化的金属在焊缝底部汇聚结合形成焊核区,此区域中观察不到明显的标示材料。焊核区金属挤压周边变形金属,受远处母材的阻碍作用而向上迁移,到达焊缝上部时受轴肩挤压作用,焊核区两侧变形金属最终在紊流区汇聚,标示材料清晰可见。轴肩区金属直接与搅拌头接触,塑化程度较紊流区的要好。此外当偏心距较小时,搅拌针的搅拌作用较差,塑化金属向下迁移量及沿搅拌针两侧往后迁移的金属量较少,焊核区尺寸较小,紊流区内出现疏松孔洞。增加搅拌针偏心距,搅拌头的搅拌作用明显加强,塑化金属向下迁移量及沿两侧迁移的金属量变多,焊核区尺寸也随之增加,焊核区金属对周边金属挤压力更大,周边金属变形程度更大,横向迁移距离更宽而使得焊核区宽度变大。但继续增加偏心距至 0.4 mm 时,搅拌针的搅拌效果反而变差,塑化金属迁移量降低,焊核区尺寸随之减小。

由此认为,焊缝底部塑化金属向周围迁移距离不仅受搅拌针挤压力作用,还受周边金属温度分布及其变形抗力影响^[10]。当偏心距太小,搅拌针破碎金属效果太差,周围金属温度太低,变形抗力较大,

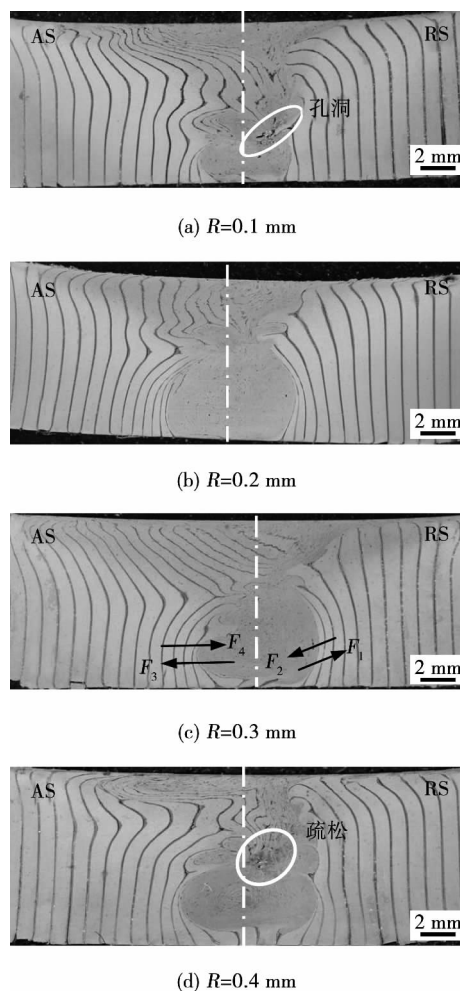


图 6 不同偏心距搅拌头下获得的焊缝横截面形貌(沿水平方向上)

Fig. 6 Cross sections of welds produced by tool pins with different eccentricities(along horizontal direction)

向下迁移金属量少且向周围迁移距离小。而偏心距太大,搅拌针搅拌效果过于剧烈,单位时间内摩擦产热过大,焊缝上层金属温度过高而使得塑化金属向下迁移量急剧减少。且焊缝底部金属温度相对较低,变形抗力大,焊缝底部塑化金属无法挤压周边金属横向移动而更容易沿着搅拌针表面向上回流。此时又由于轴肩区金属温度过高,对向上回流的塑化金属顶锻力较小,导致向上迁移的塑化金属溢出轴肩,此区域内没有足够的塑化金属填充而导致疏松孔洞缺陷产生。

2.4 焊缝塑性金属流动模型建立

根据上述焊缝金属塑性流动形态分析与讨论,建立了其塑性流动物理模型,如图 7 所示。图 7a 表示为焊接时搅拌头波动式挤压金属流动模型,图 7a 中 ω 表示搅拌头旋转方向,最外围大圆圈为轴肩覆盖区,内部小圆代表搅拌针静态轨迹,外围虚线为焊接时搅拌针的实际动态运动轨迹。图 7b 表示为搅

拌头旋转一周内搅拌针所处的4个典型位置,两中心线间距 r 表示搅拌针偏心距,虚线圆圈为搅拌针的静态位置,实线圆圈为搅拌针旋转时的位置, L_1 表示为搅拌针长轴半径,而 L_2 则代表短轴半径.位置1为搅拌针圆心偏向搅拌头正后方,位置2为圆心偏向前进侧,位置3为圆心处于搅拌头正前方,位置4则为圆心偏向焊缝后退侧.

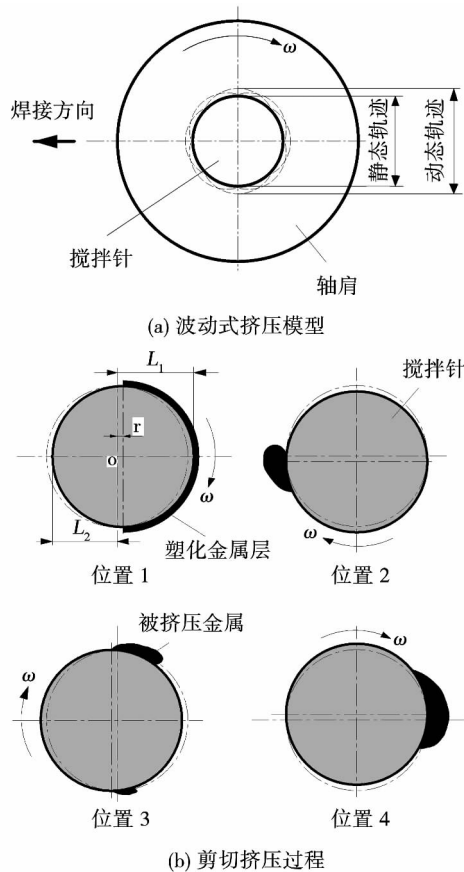


图7 搅拌针波动式挤压塑性流动物理模型

Fig. 7 Physical model of plastic flow by wave extruding of tool pin

搅拌摩擦焊接过程中,高速旋转的搅拌针剪切下一层薄的塑化金属,并随着搅拌针旋转方向开始运动.当搅拌针从位置1旋转至位置2时,搅拌针长轴向焊缝前进侧方向运动,挤压塑化金属向前侧移动,绝大部分金属被搅拌针挤压向前流动,搅拌头后方留下空隙,周围的变形金属有一个反向朝空腔中挤压的趋势.当搅拌针从位置2向位置3旋转时,搅拌针从前进侧向搅拌头正前方挤压,受到偏心力的作用,塑化金属绕过搅拌针向两侧挤压,一部分金属顺着搅拌头旋转方向流向返回侧,一部分金属流向前进侧搅拌头后方填充留下的空腔.当搅拌针从位置3到位置4运动时,塑化金属逐渐填满搅拌

头后方的空腔,部分塑化金属顺着搅拌针从返回侧流向前侧.当搅拌针从位置4向位置1运动时,搅拌针再次剪切下塑化金属层,依次重复上述过程,搅拌针经历无数个波动式的挤压过程形成最终的焊缝.焊接过程中,通过多次周期挤压形成金属层,各金属层之间的相互叠加形成焊缝,并在横截面上显示出洋葱环结构.当搅拌针偏心距太小时,搅拌偏心力太弱,剪切并挤压焊缝的金属量较少而导致无法填满空腔,就会出现图4a中的孔洞缺陷.当偏心距太大时,搅拌针偏心剪切作用太强,焊缝上部部分金属可能处于熔化状态,导致搅拌针与塑化金属出现滑动摩擦,对沿搅拌针螺纹表面往上回流的塑化金属的挤压力迅速降低,导致焊核区尺寸不增反降.

3 结 论

(1) 在搅拌摩擦焊缝横截面沿厚度方向上形成一个新的“紊流区”,这是由于焊缝上方轴肩区和下方焊核区共同挤压塑性金属迁移所造成的结果,且前进侧挤压区变形金属尺寸均大于返回侧.

(2) 随偏心距增加,焊核区面积、宽度及其两侧标示材料向上迁移最大高度呈先增大后减小的趋势,前进侧材料向上迁移的最大高度始终大于返回侧.其中采用偏心距为0.2 mm搅拌头焊接时获得的焊核区面积及两侧变形金属向上迁移高度最大,而焊核区最大宽度则由0.3 mm偏心距搅拌头获得.

(3) 搅拌针偏心距大小决定单位时间内焊缝金属的剪切挤压量及温度变化,从而影响搅拌针通道内向下迁移塑性金属量.偏心距太小或太大时,焊缝中均易出现疏松孔洞缺陷.

(4) 搅拌针偏心挤压是导致焊缝成形不一的主要原因.通过波动式挤压模型能更直观地反应单个周期内塑性金属剪切、挤压及其流动过程.

参考文献:

- [1] Canaday Clinton T, Moore Matthew A, Tang W, et al. Through thickness property variations in a thick plate AA7050 friction stir welded joint [J]. Materials Science and Engineering A, 2013, 559(8): 678-682.
- [2] Nandan R, Debroy T, Bhadeshia H. Recent advances in friction-stir welding process, weld joint structure and properties [J]. Progress in Materials Science, 2008, 53: 980-985.
- [3] Xu W F, Liu J H, Zhu H Q, et al. Influence of welding parameters and tool pin profile on microstructure and mechanical properties along the thickness in a friction stir welded aluminum alloy [J]. Materials and Design, 2013, 47: 599-606.

- [4] Mishra R S , Ma Z Y. Friction stir welding and processing [J]. *Materials Science and Engineering R*, 2005 , 50: 1 - 78.
- [5] 柯黎明,潘际奎,邢 丽,等. 搅拌针形状对搅拌摩擦焊缝截面形貌的影响[J]. *焊接学报*, 2007 , 28(5): 16 - 20.
Ke Liming , Pan Jiluan , Xing Li , *et al.* Influence of pin shape on weld transverse morphology in friction stir welding [J]. *Transactions of the China Welding Institution*, 2007 , 28(5): 16 - 20.
- [6] 王晓东,柯黎明,邢 丽,等. 搅拌针表面螺纹头数与轴肩下压量对金属轴向迁移的影响[J]. *中国有色金属学报*, 2012 , 20(1): 100 - 105.
Wang Xiaodong , Ke Liming , Xing Li , *et al.* Effects of thread number of stirring pin and pluge depth on transfer of metal in weld thickness direction [J]. *The Chinese Journal of Nonferrous Metals*, 2012 , 20(1): 100 - 105.
- [7] Thomas W M , Nicholas E D. Friction stir welding for the transportation industries [J]. *Materials and Design*, 1997 , 18: 269 - 273.
- [8] Khodaverzideh H , Heidarzadeh A , Saeid T. Effect of tool pin profile on microstructure and mechanical properties of friction stir welded pure copper joints [J]. *Materials and Design*, 2013 , 45: 265 - 270.
- [9] Mao Y Q , Ke L M , Liu F C , *et al.* Effect of tool pin eccentricity on microstructure and mechanical properties in friction stir welded 7075 aluminum alloy thick plate [J]. *Materials and Design*, 2014 , 62: 334 - 343.
- [10] 柯黎明,潘际奎,邢 丽,等. 搅拌摩擦焊缝金属塑性流动的抽吸-挤压理论 [J]. *机械工程学报*, 2009 , 45(4): 89 - 94.
Ke Liming , Pan Jiluan , Xing Li , *et al.* Sucking-extruding theory for the material flow in friction stir welds [J]. *Journal of Mechanical Engineering*, 2009 , 45(4): 89 - 94.
- [11] Fu R D , Sun Z Q , Sun R C. Improvement of weld temperature distribution and mechanical properties of 7050 aluminum alloy butt joints by submerged friction stir welding [J]. *Materials and Design*, 2011 , 32: 4825 - 4831.

作者简介: 毛育青,男,1987 年出生,博士. 主要从事轻合金搅拌摩擦焊、激光焊及 3D 打印、金属基复合材料制备等研究工作. 发表论文 20 篇. Email: maoyuqing-8888@163.com

通讯作者: 柯黎明,男,博士,教授,博士研究生导师. Email: liming_ke@126.com

[上接第 50 页]

- [5] 郝建军,赵建国,彭海滨,等. 氩弧熔覆 WC 增强镍基涂层的组织与性能分析[J]. *焊接学报*, 2009 , 30(12): 26 - 28.
Hao Jianjun , Zhao Jianguo , Peng Haibin , *et al.* Microstructure and properties of WC particulate reinforced Ni-based composite coatings formed by argon-arc cladding [J]. *Transactions of the China Welding Institution*. 2009 , 30(12): 26 - 28.
- [6] 于琳华,殷秋菊,林东玲. 表面强化技术在模具中的应用与发展[J]. *热处理技术与装备*, 2009 , 30(2): 5 - 8.
Yu Linhua , Yin Qiuju , Lin Dongling. Application and development of surface hardening technology in the die [J]. *Heat Treatment Technology and Equipment*, 2009 , 30(2): 5 - 8.
- [7] 潘继岗,樊自拴,孙冬柏,等. 轧辊修复技术的研究现状和展望[J]. *新技术新工艺*, 2005 (3): 60 - 62.
Pan Jigang , Fan Zisuan , Sun Dongbai , *et al.* Present state and perspectives of roller repaired technology , 2005(3): 60 - 62.
- [8] Picas J A , Xiong Y , Punset M , *et al.* Microstructure and wear resistance of WC-Co by three consolidation processing techniques [J]. *International Journal of Refractory Metals and Hard Materials*, 2009 , 27(2): 344 - 349.
- [9] 朱润生. 自熔合金粉末的研究[J]. *粉末冶金工业*, 2000 , 10(2): 7 - 14.
Zhu Runsheng. Investigation of self-fluxing alloy powders [J]. *Powder Metallurgy Industry*, 2000 , 10(2): 7 - 14.

作者简介: 赵洪运,男,1966 年出生,博士,教授,博士研究生导师. 主要从事先进材料焊接工艺及装备. 发表论文 30 余篇. Email: zhaohy6691@163.com

通讯作者: 张连旭,男,硕士. Email: zhanglianxu1989@163.com

ing , Hebei University of Science and Technology , Shijiazhuang 050018 , China) . pp 41 - 46

Abstract: Based on separability of plasma arc , the twin-body plasma arc was established as the wire was the guided electrode. Combined with electrical signals and droplet transfer behavior of different welding parameters , the droplet transfer behavior under different bypass modes was analyzed. The results showed that as the bypass mode was constant current mode , the droplet achieved steady and rapid transition as the bypass current increased , the transition frequency increased as the wire feed speed increased. But when the wire feed speed was too fast , the wire passed through the plasma arc without forming droplet. With the change of the bypass current and wire feed speed , the bypass voltage and the plasma arc voltage occurred significant fluctuations , but the bypass current and the plasma arc current remained stable , the bypass voltage increased as the plasma voltage dropped. As the bypass mode was constant voltage mode , droplet achieved stable and rapid transition as the bypass voltage and wire feed speed increased , losing its stability as the overloaded voltage was set. With the change of the bypass voltage and wire feed speed , the bypass current was increased as the bypass voltage increased , but the plasma arc voltage , the voltage bypass , the bypass current , and even the plasma current showed significant volatility.

Key words: twin-body plasma arc; bypass arc; droplet transfer; constant voltage mode; constant current Mode

Process research of Co-based coating on Q235 steel by PTAW ZHAO Hongyun¹ , TIAN Ze¹ , HE Wenxiang¹ , ZHANG Lianxu² (1. Shandong Provincial Key Laboratory of Welding and Joining , Harbin Institute of Technology , Weihai 264209 , China; 2. Dongfeng Motor Company , Manufacturing Technology Department of Dongfeng Nissan Passenger Vehicle Company Headquarters , Guang Zhou 510800 , China) . pp 47 - 50 , 56

Abstract: It can be found that improving the wear and corrosion resistance properties of workpiece is one of the most important methods to enhance its life in terms of the damages of mechanical equipment in die industry and metallurgy. The PTAW deposited resistance overlays is the key direction at present. In present paper , the Co-based self-fluxed high-temperature alloy coatings were fabricated with the method of orthogonal experiment by using PTAW process , the relationship between the mass energy and the dilution rate is discussed. The influence of process parameters on deposited overlays. The influence of three parameters welding current , welding speed and feeding rate on hardness , wear resistance and dilution rate of the coatings was explored in detail. Optimal parameters for wear resistance coating is given as below: spray current is 60 A , powder flow is 23.5 g/min and welding speed is 80 mm/min.

Key words: PTAW; process optimization; surface properties

Effect of pin eccentricity on flow behavior of plastic material in friction stir welds MAO Yuqing^{1,2} , KE Liming^{1,2} , LIU Fencheng¹ , LIU Qiang² (1. National Defence Key Discipline Laboratory of Light Alloy Processing Science and Technology , Nanchang Hangkong University , Nanchang 330063 , China; 2. State Key Laboratory of Solidification Processing , Northwestern Polytechnical University , Xi'an 710072 , China) . pp 51 - 56

Abstract: Four tools with a pin eccentricity of 0.1 , 0.2 , 0.3 and 0.4 mm were designed to friction stir weld lamination by inserting tracer material , and effect of pin eccentricity on metal flow behavior of the weld was studied. The results showed that , the cross section of the weld consisted of shoulder zone , turbulent flow zone , nugget zone and extruded zone , and the formation of the turbulent flow zone was contributed to combined extruding action of nugget zone and shoulder zone. Moreover , the size of deformed metals on the AS is larger than on the RS. In the same welding conditions , with increasing pin eccentricity , the area and width of nugget zone increased firstly and then decreased. The changing trend of transfer height of insert tracer materials was similar , and the maximum transfer height on the AS was bigger than on the RS. The area of nugget zone and the transfer height of insert tracer material were produced by a tool pin with an eccentricity of 0.2 mm. But the maximum width of nugget zone was obtained by a tool pin of 0.3 mm eccentricity. According to the three-dimensional plastic flow of the weld metal , a wave extruding physical model of the pin was proposed.

Key words: friction stir welding; pin eccentricity; plastic flow; wave extruding model

Microstructure of TA15 alloy and 18-8 stainless steel joint by TIG with filler metal LIU Kun , LI Yajiang , WANG Juan , LAN Yazhou (Key Laboratory for Liquid-Solid Structural Evolution and Processing of Materials , Ministry of Education , Shandong University , Jinan 250061 , China) . pp 57 - 60

Abstract: TA15 titanium alloy and 18-8 stainless steel were welded by tungsten inert-gas arc welding with copper alloy as filler metal. Microstructure , phase constituents , elements distribution and microhardness near the fusion zone of TA15 alloy / 18-8 stainless steel joint were investigated by optical microscope , scanning electron microscope , electron probe microanalysis and microhardness tester. Results indicated that the molten unmixed zone near TA15 alloy side primarily included α -Ti , brittle phosphide (Ti_3P) and $Ti(Cu, Fe)$, while the fusion zone near 18-8 stainless steel was mainly composed of Fe-P eutectic microstructure. The enrichment of P in the fusion zone near 18-8 stainless steel contributed to the forming of eutectic microstructure. The residual Cu formed the clump zone. The microhardness of fusion zones was obviously higher than that of heat affected zone and weld metal. Brittle Ti_3P phase resulted in the highest microhardness of molten unmixed zone near titanium alloy reaching 720 $HV_{0.5}$.

Key words: TA15 titanium alloy; 18-8 stainless steel; tungsten inert-gas arc welding with filler metal; microstructure

Effect of protection condition on forming and performance of weld in titanium alloy laser-TIG hybrid welding SHI Jipeng , WANG Hongyang , YANG Linbo , LIU Liming (Key Laboratory of Liaoning Advanced Welding and Joining Technology , Dalian University of Technology , Dalian 116024 , China) . pp 61 - 65

Abstract: Laser-TIG hybrid experiments were carried out for butt weld of the TA15 titanium alloy sheets with 2.5 mm thick. Multifunction tensile testing machine , infrared thermometer , EPMA and SEM were used to analyze the weld joints , and a comparison with single TIG was made. Welding process , joint performance and weld protection were investigated. Results show that compared with single TIG welding , when full penetration